

RESEARCH PAPER

Investigating Thermophysical Properties and Thermal Performance of Al_2O_3 Nanoparticles in Water and Ethylene Glycol Based Fluids

Bahman Rahmatinejad

Department of Mechanical Engineering, Technical and Vocational University (TVU), Tehran, Iran

ARTICLE INFO

Article History:

Received 05 March 2022

Accepted 21 June 2022

Published 01 July 2022

Keywords:

Al_2O_3

Nano-fluid

Nanoparticles

Thermal Conductivity

Thermo-physical Properties

ABSTRACT

In this study, the thermo-physical properties and thermal performance of Al_2O_3 nanoparticles were experimentally investigated in water-based fluid and ethylene glycol, and nanoparticles were produced by PNC1k-C device by electric explosion method. In order to measure the thermal conductivity, diameter and viscosity of the obtained nano-fluids, hot wire method (KD2-Pro device), dynamic light scattering (DLS) and Ostwald viscometer ASTM D445-06 were used respectively. The temperature range of the experiments was between 20 degrees to 50 degrees. The results showed that adding 1% by weight of sodium dodecyl gasoline sulfonate (SDBS) to $\text{Al}_2\text{O}_3 + \text{H}_2\text{O}$ stabilizes this nano-fluid for 22 days. In this case, the zeta potential is 37.7 mv, which indicates good nano-fluid stability. The results showed that with increasing the volume fraction of nanoparticles in the base fluid, the thermal conductivity, density, steam pressure and slope of the heating curve increase and the surface tension decreases. With increasing temperature, thermal conductivity and specific heat of water increased and density, viscosity and specific heat of nano-fluid decreased with different volume fractions. Also, with increasing the diameter of nanoparticles, the thermal conductivity decreased and the surface tension of the nano-fluid increased. The stronger the thermal properties of the base fluid, the greater the effect on the thermal conductivity of the nano-fluid. The obtained practical thermal conductivity coefficient was compared with the values of the prediction models of this coefficient. Based on the regression obtained for the calculated experimental results ($R = 0.99$), this value is consistent with the Timofeeva model.

How to cite this article

Rahmatinejad B. Investigating Thermophysical Properties and Thermal Performance of Al_2O_3 Nanoparticles in Water and Ethylene Glycol Based Fluids. J Nanostruct, 2022; 12(3):642-659. DOI: 10.22052/JNS.2022.03.018

INTRODUCTION

One of the most important ways to reduce energy consumption in various industries is to increase thermal efficiency. So that the limitation of fluid heat transfer has led to the loss of a large part of energy. This weak thermal conductivity has led to improved heat transfer of operating fluids as a new method of advanced heat transfer. So the

idea of dispersing solid particles in fluids, which started with millimeters and micrometers, was completed with the use of solid nanoparticles, and today nano-fluids are a good alternative to normal fluids such as water and oil. Nanoparticles cause a significant increase in the heat transfer of nano-fluids. The interesting properties of nanofluids and their great potential for increasing heat transfer

* Corresponding Author Email: brahmati@tvu.ac.ir



caused this group of fluids to be considered by researchers in recent years. The addition of nanoparticles to the base fluid has a significant effect on the thermal conductivity coefficient and this has been considered by researchers [1,2]. Various studies have been performed on the parameters affecting the heat transfer of Al_2O_3 nano-fluid, some of which are mentioned below. Das et al. studied the behavior of water and copper oxide Nanofluid as well as water and aluminum oxide with changing temperature. They concluded that by increasing temperature, the thermal conductivity of nanofluid increases [3]. Cheng Sung et al. investigated the overall heat transfer coefficient of alumina-water nanofluid in multi-channel heat exchanger. They observed that at a constant amount of heat (120 w), as the mass flow and concentration of the nanoparticles increases, the ratio of the total heat transfer coefficient of the nanofluid to water increases [4]. Ismaeilzadeh et al. investigated the properties of heat transfer and hydrodynamic of flow with aluminum oxide nanoparticles experimentally inside a flat tube. The results showed that increasing the particle volume fraction leads to an increase in the heat transfer coefficient [6]. In a study by Peygambarzadeh et al., the changes in the heat transfer coefficient of $Al_2O_3 + H_2O$ nanofluid displacement in a car radiator was investigated. According to their observations, by increasing temperature, Reynolds number and concentration, the heat transfer coefficient of nanofluid also increases [7]. Timah and Moglani studied the effect of a magnetic field on a square chamber filled with nanofluids. The results showed that when a weak magnetic field is applied, adding the percentage of nanoparticles is necessary to increase heat transfer but under strong field, it is not appropriate [8]. Zeitun and Ali studied in vitro the heat transfer caused by the impact of the water- aluminum nanofluid circular jet on a circular target plane and investigated the influence of parameters such as fluid flow rate, nozzle diameter, target plate diameter and volume fraction of the nanoparticles. They concluded that by increasing the volume fraction of nanoparticles in the constant Reynolds, the Nusselt number increases [9]. Ambomuzi and Flip investigated the effect of nanofluid surface charge on thermal conductivity. They used three types of surface active agents, one negative, one positive and one non-ionic, in aluminum-water nanofluid. The

results showed that the use of ionic surface active factors has a positive effect on the dispersion and non-deposition of nanoparticles in nanofluids but did not have a significant effect on the thermal properties of nanofluid [10]. Siam Sandar et al. Showed that the viscosity of nanofluids depends on the particle concentration, temperature, particle size and shape, and the viscosity of the base fluid. In addition to the above, the way of nanofluid stabilization, the way of making and synthesis of nanoparticle and the nanoparticle manufacturer, are effective in the viscosity of nanofluids [11]. Mina and colleagues investigated the viscosity of nano-fluid $Al_2O_3 + H_2O$ for temperature of 20 to 70 ° C, nanoparticles volume concentration between 1% and 9%, and nanoparticles between 13 nm and 131 nm [12]. Mostafizor et al. investigated the changes of Al_2O_3 nanofluid viscosity with temperature. The results show that increasing the temperature affects the Brownian motion of the nanoparticles and also decreases the adhesion of the liquids, thus increasing the temperature decreases the viscosity of the nanofluids [13]. Khodaei showed, the mechanochemical reaction of a non-stoichiometry Fe_2O_3-Al system ($Fe_2O_3+Al+Fe$ powder mixture) was performed to produce the Fe_3Al-30 vol.% Al_2O_3 nanocomposite. The progress of the reaction was followed by X-ray diffractometry (XRD) and transmission electron microscopy (TEM). XRD analysis of mechanochemically synthesized Fe_3Al-30 vol.% Al_2O_3 nanocomposite showed no evidence of the produced Al_2O_3 phase, whereas TEM analysis revealed the crystalline Al_2O_3 phase. The X-ray absorption by component higher mass absorption coefficient (Fe_3Al matrix) in highly strained nanocomposite leads to a decrease in the diffraction intensity of components with lower mass absorption coefficient and with low volume fraction (Al_2O_3). High-temperature heat treatment lead to crystallite growth as well as lattice strain reducing, which resulted in the capability of detection of Al_2O_3 by XRD analysis. [14]. Hemmat Esfah and Saad al-Din reported in their study that at higher volume fractions, the effect of temperature on thermal conductivity coefficient is greater [15]. In another study, Hemat Esfah showed that different surfactants were used depending on the active surface of the nanoparticles, which inaccuracy in the choice of surfactant type may lead to further aggregation of the nanoparticles. Thus the choice of surfactant is

dependent on both the base fluid and the material of the nanoparticles [16]. Using the classical Nusselt layer condensation theory, Turkilmas Oglu presented two different analytical models for nanofluids. In this analysis, he used silver, copper, copper oxide, aluminum oxide, and titanium oxide nanoparticles with water-based fluid. His results show that as the volume fraction of nanoparticles increases, the thickness of the condensed layer decreases as well as the heat transfer increases [17]. Bashir et al. Showed, series of Copper Ruthenium (Cu-Ru) bimetallic catalysts supported on $\gamma-Al_2O_3$ with different metal loading are prepared and investigated for catalytic wet air oxidation of ammonia to nitrogen. The ammonia decomposition activity was studied at three different temperatures i.e. 150 °C, 200 °C, and 230 °C and it is found that catalytic activity increases with the increase in temperature along with the high selectivity towards nitrogen production. The results also revealed that the bimetallic Cu-Ru/ $\gamma-Al_2O_3$ are much more efficient especially stable than the corresponding monometallic Cu and Ru catalysts. Up to 99 % ammonia decomposed to N_2 without any undesirable nitrites and nitrates at 230 °C by optimizing catalysts to ammonia ratio [18]. Ghiyasiyan et al. Have worked on the morphology and different sizes of AlV3O9 structures used in rechargeable battery technologies [44]. Davoodabadi Farahani et al. investigates experimentally heat transfer of the forced convection boiling of a R134a/nano oil mixture in a horizontally-aligned tube with an aluminum helical fin. The effects of various parameters including refrigerant mass flow, vapor quality, star-shaped fin, oil concentration and volume fraction of nanoparticles are studied. SiO_2-TiO_2 nanoparticles are synthesized by applying both ultra-sound irradiation and sol-gel methods. The findings indicate that as the mass flow enhances, the heat transfer coefficient rises. The heat transfer coefficient and pressure drop have increased by using a helical fin. Regarding the oil-refrigerant mixture, the heat transfer coefficient augments at low vapor quality and reduces at high vapor quality. By adding nanoparticles, heat transfer increases, but a decreasing trend in heat transfer is observed from a certain vapor quality. The highest percentage of increase in heat transfer at a mass velocity of 380 kg/m².s is for the case with a fin and a mixture of R134a/nano oil, and this amount is equal to 89% [45]. The use of

nanofluids as a fluid with advanced heat transfer characteristics is increasing in various industries. Therefore, it is important to determine the thermophysical properties of these fluids. Due to the lack of comprehensive studies in this regard and the inefficiency of classical relationships in precisely determining the thermal conductivity coefficient of nanofluids and on the other hand, presenting contradictory results in this case causes to this research to be conducted. Therefore, these properties were determined in vitro and compared with reliable sources to evaluate the accuracy of the obtained results. The main purpose of this study is to investigate the thermo-physical properties and thermal performance of Al_2O_3 nanoparticles in water and ethylene glycol at different temperatures and volume fractions.

MATERIALS AND METHODS

Preparation of nano-fluids

In this research, first, Al_2O_3 nanoparticles were produced by PNC1k-C device of Payam Avaran Nanotechnology Company of Fardanegar by electric explosion method in the form of metal nano-colloids. Al_2O_3 was prepared with a purity of over 99%. Al_2O_3 nanoparticles have successfully been synthesized by using a sol-gel method. TEM (Transmission electron microscope) and SEM (Scanning Electron Microscope) images were taken to obtain the structure and morphology of nanoparticles produced from nanoparticles. TEM images were taken by H9500 transmission electron microscope and SEM images were taken by HITACHI Su3500 scanning electron microscope (Fig. 1).

The chemical compositions of the present Al_2O_3 sample after annealing were determined by EDS and shown in Fig. 1 with reference peak at 0 Kev. Spectrum study reveals the presence of aluminium and oxygen elements with 38 and 62 atomic weight percentages without impurities and it confirms the stoichiometry of aluminium oxide nanomaterials synthesized by the co-precipitation method (Fig. 1).

Dynamic Light scattering (DLS) and X-ray diffraction (XRD) were used to measure the nanoparticle diameter. In the DLS method, a laser beam is emitted into the suspension and the scattering of the laser light is recorded by an optical detector. Particles of different sizes scatter light in different ways. Larger particles scatter light at smaller angles, while smaller particles

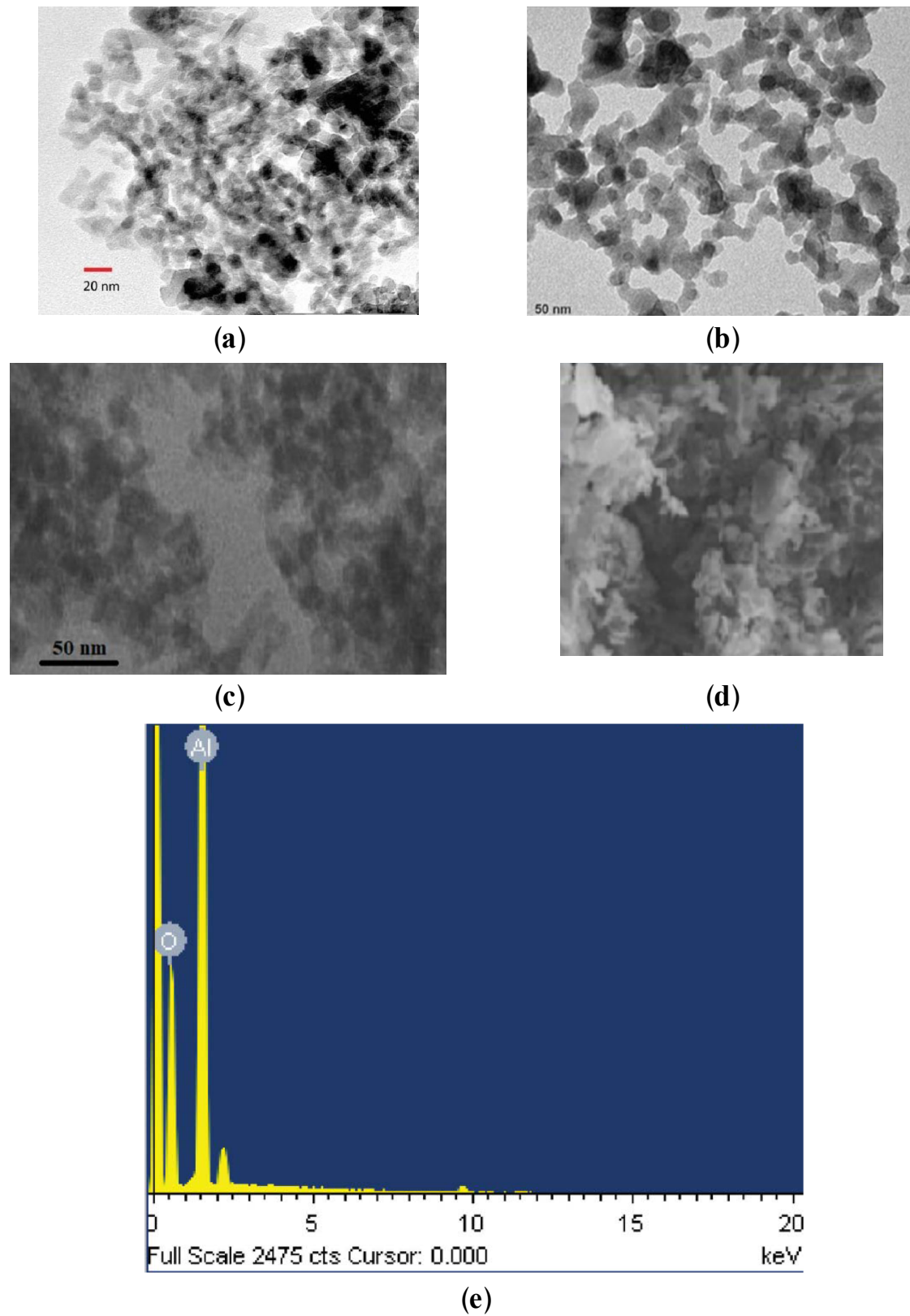


Fig. 1. Image of Al_2O_3 nanoparticles (a) TEM 20 nm, (b) TEM 50 nm, (c) SEM 50 nm, (d) SEM 20 nm, (e) EDS spectrum of Al_2O_3

scatter light at wider angles. The scattering of light by solid particles creates a pattern of light and dark spots on the detector. These light and dark patterns change with the motion of the particles, and cause to change the created pattern over time. The DLS device software can determine the particle size distribution by examining changes in this pattern over time. Larger particles have a lower velocity in solution than smaller particles. Hence, the diffraction pattern changes more slowly in a suspension with larger particles than in a suspension with smaller particles. The relationship between particle size and Brownian motion speed is established by the Stokes Einstein relation:

$$d_H = \frac{KT}{3\pi\eta D} \quad (1)$$

d_H: Hydrodynamic Diameter of Particle, K: Boltzmann constant, η : solvent viscosity that depends on temperature and is not related to system density and pressure. T: Absolute temperature and D: Influence coefficient [5]. Max von Laue, in 1912, discovered that crystalline substances act as three-dimensional diffraction gratings for X-ray wavelengths similar to the spacing of planes in a crystal lattice. X-ray diffraction is now a common

technique for the study of crystal structures and atomic spacing. X-ray powder diffraction (XRD) is also utilized to study the surface property. This analysis will enlighten about the crystallinity or the amorphous nature of the testing materials. For the XRD analysis, very small amount of material is utilized of an order of 0.2 g, which is finely powdered and consistently dispersed on the testing plate. For the analysis, diffractometers utilize different radiations such as Cu-Kα radiation with a wavelength of 1.54 Å. The angle 2θ in the setup of the XRD fluctuate in a range of 10–90 degrees at a measurable step of 0.01 degrees. The analysis of the XRD is on the basis of the peak observed. If a sharp peak is observed, it infers a crystalline nature; otherwise, an amorphous nature of the surface is inferred (Fig. 2). In the XRD diffraction method, to determine the size of the nanoparticles, the processing and analysis of the X-ray return from the sample surface is examined. In the XRD method, the particle size is calculated from Equation 2.

$$D = \frac{0.93 \lambda}{K \cos \theta_B} \quad (2)$$

K: Shape coefficient (for spherical nanoparticles)

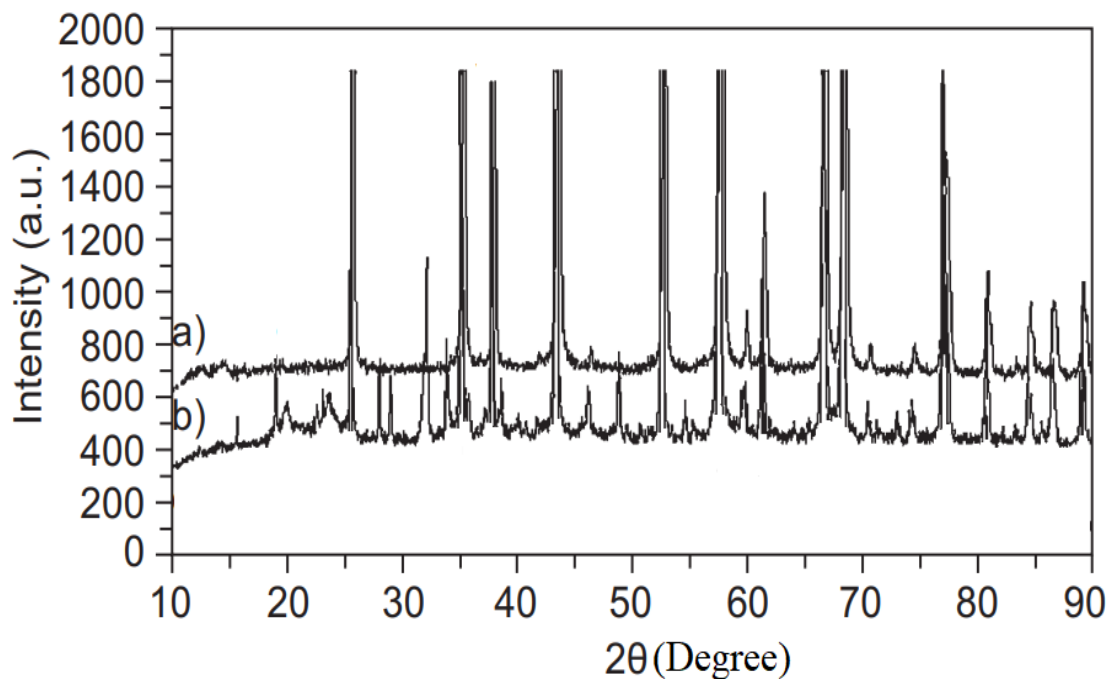


Fig. 2. XRD At 1200 ° C (a) No sulfonate, (b) With SDBS sulfonate

K = 0.93), λ: X-ray wavelength, D: Particle diameter, B: Maximum peak width at half height, θ: The scattering angle for which the maximum peak is formed.

FT-IR spectra were obtained using a Perkin-Elmer spectrometer at a resolution of 8 cm⁻¹. It is now possible to detect the presence of transition Al₂O₃ and perhaps their nature on oxide scales formed by oxidation of alumino-former alloys. For this purpose, PM2000 samples, oxidized at different temperatures (from 973 K to 1373 K in air for 7 hours) were studied by IR spectroscopy. FT-IR spectra are reported in Fig. 3.

An electric mixer with the ability to adjust the speed from 200 to 3000 rpm was used to prepare the nano-fluid. Then a magnetic shaker was used with a speed of 100 to 2000 rpm and a heating power of 400 W. In order to maintain the stability of the solution to be suitable for engineering works, 1% by weight of surfactants (sodium dodecyl benzene sulfonate) was used. The characteristics of surfactants are given in Table 1.

The mass of nanoparticles (m_p) and the mass of the base fluid (m_f) were measured accurately (0.01 g). Equation 3 can be used to estimate the weight percentage [28].

$$\phi = \left(\frac{m_p}{m_p + m_f} \right) \times 100 \quad (3)$$

If we show the density of nanoparticles (ρ_{np}) and the density of the base fluid with (ρ_{bf}), we can estimate the volume concentration of nanoparticles in the base fluid from relation 4 [36].

$$\text{Volume Concentration } (\varphi) = \left[\frac{\frac{W_{np}}{\rho_{np}}}{\frac{W_{np}}{\rho_{np}} + \frac{W_{bf}}{\rho_{bf}}} \right] \times 100$$

In relation 4 the bf index is for the base fluid

and np for the nanoparticles.

Measurement of Nanofluid Thermal Conductivity Coefficient

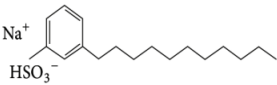
Methods of Estimating Thermal Conductivity Coefficient

Numerous experimental relationships have been proposed to measure the thermal conductivity by theoretical methods. To estimate the thermal conductivity, static and dynamic models have been proposed by various researchers. In this study, due to the fact that this coefficient has been calculated in practice, static models were used only to evaluate the results. In addition to the need for lower parameters to obtain thermal conductivity, these models also show good agreement with laboratory results in low volume fraction. These models are provided in Table 2.

Determination of Thermal Conductivity Coefficient Using Transient Hot Wire Method

The transient hot wire method is widely used for the experimental measurement of the thermal conductivity coefficient of liquids statically and with a linear source. A thin metal wire made of platinum (or tantalum with a diameter of 5-80 μm) is placed inside the liquid, which acts as both a heat source and a thermometer. The thermal conductivity coefficient of the test specimen can be obtained by changing the temperature of the hot wire over a period of time. The thermal resistance of the wire changes with temperature. A wheatstone bridge is used to measure the electrical resistance of the R_w wire. The electrical resistance of R₃ potentiometer is set when the galvanometer G shows zero current. When the bridge is balanced with zero galvanometer flow, the value of R_w can be determined according to the known values of R₁, R₂ and R₃.

Table.1. Specifications of surfactants.

sulfonate	Molecular formula	Formula structure	Molecular Weight (g/mol)	Density ($\frac{g}{cm^3}$)
Sodium dodecyl benzene sulfonate [43]	C ₁₈ H ₂₉ NaO ₃ S		348.48	1.02

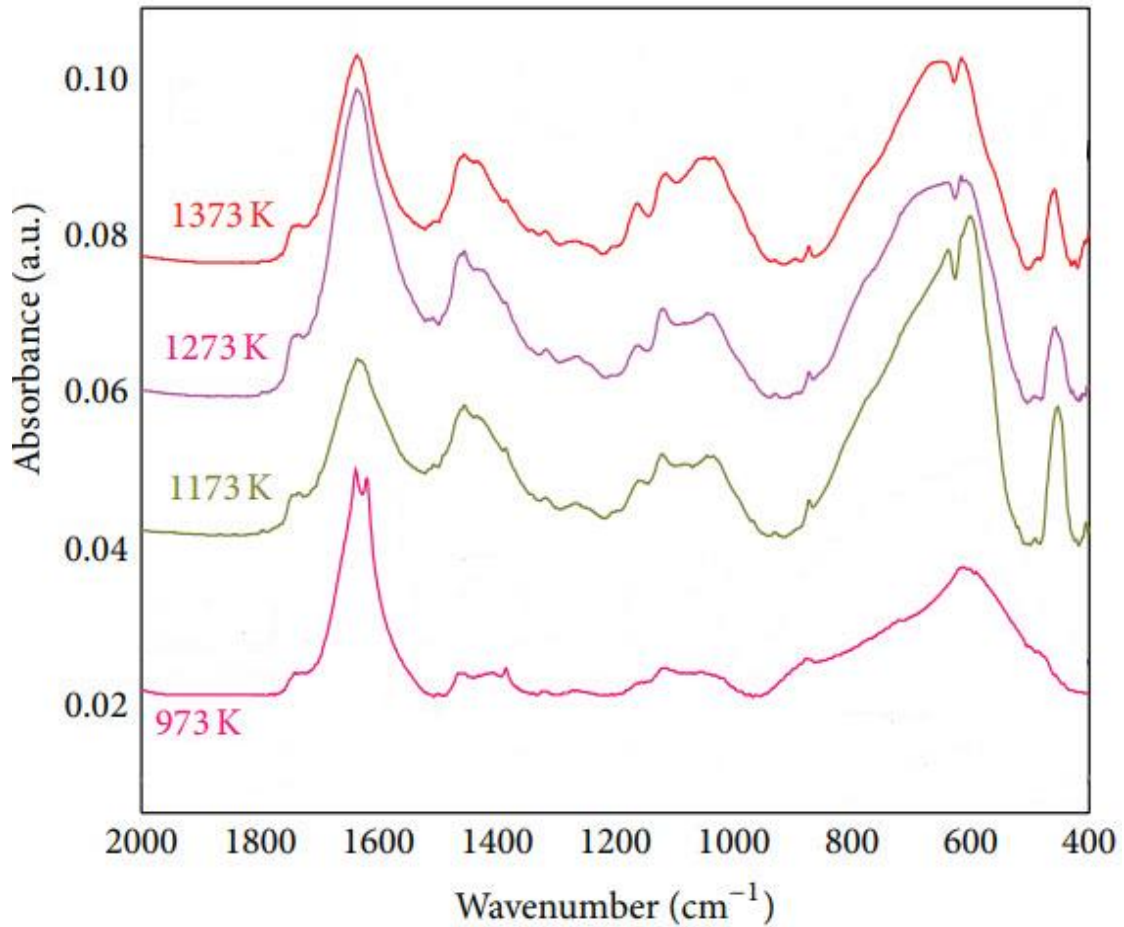


Fig. 3. FTIR spectra of oxidized PM2000 at various temperatures from 973 K to 1373 K.

$$R_w = \frac{R_1 R_2}{R_3} \quad (5)$$

Since nanofluids are conductors of electric current, if a thin layer of electrical insulation is used to cover the platinum wire, it will prevent the problems such as creating an electric current in the fluid that generates heat in the wire. This technique, called modified transient hot wire, was developed by Nagasaka and Nagashima. They used epoxy adhesive layer to cover the wire [28]. Due to the very small diameter of the platinum wire and its high electrical conductivity, it can be considered as a linear source in an unlimited cylindrical environment. In this study, the relationships presented in Source 29 were used. Transient temperature for a long time follows the following relationship.

$$T(r,t) = \frac{Q}{4\pi k} \left[\ln\left(\frac{4\alpha t}{r^2}\right) + \frac{r^2}{4\alpha t} - \frac{1}{4} \left(\frac{r^2}{4\alpha t}\right) - \dots - \gamma \right] \quad (6)$$

In this equation:

Q: The applied power per unit length in the heat source (W/m)

k: Thermal conductivity coefficient (W/m.k)

α : Thermal distribution coefficient m/s²

r: radial position of temperature measurement

γ : The stability of Uller is $\gamma = \ln(\sigma) = 0.57721$

This approximation can be used for a linear source located within an unlimited cylindrical environment: [29].

$$\left(\frac{r^2}{4\alpha \cdot t}\right) \ll 1 \quad (7)$$

Therefore, the equation becomes as follows [29].

$$T(r,t) = \frac{Q}{4\pi k} \left[\ln\left(\frac{4\alpha t}{r^2}\right) - \gamma \right] = \frac{Q}{4\pi \lambda} \left[\ln t + \ln\left(\frac{4\alpha}{r^2}\right) - \gamma \right]$$

Therefore, the dependence of temperature on time is as follows, which we will have in two

different times: [29].

$$\Delta T = T(t_2) - T(t_1) = \frac{Q}{4\pi k} \ln\left(\frac{t_2}{t_1}\right) \quad (9)$$

By placing Q and simplifying the following equation for k is obtained [29].

$$k = \frac{Q}{4\pi [T(t_2) - T(t_1)]} \ln\left(\frac{t_2}{t_1}\right) \quad (10)$$

The transient hot wire method allows us to measure k quickly and accurately, while also reducing the unwanted effects of thermal conductivity.

The accuracy of the Hot Wire sensor was calibrated by measuring the thermal conductivity of pure water. The uncertainty of the measured

values was estimated to be ±1%.

Thermo-physical properties of nano-fluids

Assuming that the nanoparticles are well dispersed in the base fluid and that the particle concentration is uniform throughout the system, the effective physical properties of the studied mixtures can be obtained using some classical formulas commonly used for biphasic liquids. These relationships have been used to predict the properties of nano-fluids such as density, specific heat, dynamic viscosity and thermal conductivity at different temperatures and concentrations. The density of nano-fluids can be calculated according to the law of mixtures from the Pak and Chow relation [22].

Table. 2. Mathematical models for estimating thermal conductivity coefficient.

Explanations	Mathematical model	Model
Most primitive model by assuming particles in spherical shape.	$K_{eff} = \frac{K_p \phi_p (dT/dx)_p + K_b \phi_b (dT/dx)_b}{\phi_p (dT/dx)_p + \phi_b (dT/dx)_b}$	Maxwell [19]
The modified model is Maxwell and it is in good agreement with the experimental data.	$\frac{K_{nf}}{K_f} = \frac{(K_p + 2K_f) - 2\phi(K_f - K_p)}{(K_p + 2K_f) + \phi(K_f - K_p)}$	Maxwell-Garnett [20]
Applicable to spherical particles (n = 3) and cylindrical particles (n = 6)	$K_{eff} = \frac{K_p + (n - 1)K_1 - (n - 1)(K_1 - K_p)\phi}{K_p + (n - 1)K_1 + (K_1 - K_p)\phi} K_1$	Hamilton [21]
Assuming spherical and binary interaction between particles.	$K_{eff} = [1 + 3\beta\phi + (3\beta^2 + \frac{3\beta^3}{4} + \frac{9\beta^3}{16} - \frac{\alpha + 2}{2\alpha + 3} + \frac{3\beta^4}{2^6} + \dots)\phi^2]k_1$	Jeffrey [22]
Assuming spherical and non-spherical particles.	$K_{eff} = [1 + a\phi + b\phi^2]k_1$ a = 2.25, b = 2.27 for α = 10; a = 300, b = 4.51 for α = ∞	Loo – Lin [23]
In this model, the only effective parameter is the volume percentage.	$\frac{K_{nf}}{K_f} = (1 + 3\phi)$	Timofeeva [24]
In this model, the only effective parameter is the volume percentage.	$\frac{K_{nf}}{K_f} = 1 + 7.47\phi$	Pak – Cho [25]



$$\rho_{eff} = \left(\frac{m}{V}\right)_{eff} = \frac{m_b + m_p}{V_b + V_p} = \frac{\rho_b V_b + \rho_p V_p}{V_b + V_p} = (1 - \phi_p)\rho_b + \phi_p \rho_p \quad (11)$$

$$\begin{aligned} (\rho C_p)_{eff} &= \rho_{eff} \left(\frac{Q}{m\Delta T}\right)_{eff} = \rho_{eff} \frac{Q_b + Q_p}{(m_b + m_p)\Delta T} = \rho_{eff} \frac{(mC_p)_b \Delta T + (mC_p)_p \Delta T}{(m_b + m_p)\Delta T} = \rho_{eff} \frac{(\rho C_p)_b V_b + (\rho C_p)_p V_p}{\rho_b V_b + \rho_p V_p} \\ &= (1 - \phi_p)(\rho C_p)_b + \phi_p(\rho C_p)_p \end{aligned} \quad (12)$$

ρ_{eff} is the density of the nano-fluid, V_b , is the volume of the base fluid and V_p is the volume of the nanoparticles. In this regard, ϕ the volume fraction of nanoparticles, ρ density, and index p represent nanoparticles and b represents the base fluid. Most researchers use Equation 12 to determine specific heat capacity [33].

Which can be written as relation 13.

$$C_{p,eff} = \frac{(1 - \phi_p)(\rho C_p)_b + \phi_p(\rho C_p)_p}{(1 - \phi_p)\rho_b + \phi_p \rho_p} \quad (13)$$

$C_{p,eff}$ is the specific heat constant pressure of the nano-fluid, index P for nanoparticles and index b for the base fluid. Various theoretical models have been proposed to calculate the viscosity of nano-fluids, among which the Einstein model was used in this study [32].

$$\frac{\mu_{nf}}{\mu_f} = 1 + 2.5\phi \quad (14)$$

Φ is the volume fraction of nanoparticles, μ_f the dynamic viscosity of the base fluid, and μ_{nf} the dynamic viscosity of the nano-fluid. This relationship is suggested for low volume percentage spherical particles. Parameters such as the volume of nanoparticles, their size and shape, base fluid, nano-layer thickness, dispersion techniques, temperature and pH value and ocular motion of nanoparticles are involved in determining the viscosity of nano-fluids [41-37]. In order to evaluate the results of Equation (14), the viscosity of the nano-fluid was calculated experimentally by the ASTM D445-06 Ostwald viscometer. The DA130N digital portable density meter of KEM company of Japan was used to measure the density and the KRUSS K11 Tensiometer was used to measure the surface tension.

RESULTS AND DISCUSSION

Investigation of nanoparticle sedimentation in

nano-fluids

Photograph of sediment

Preparation of uniform and stable suspension has a significant effect on improving the thermal properties of nano-fluids. One of the factors that affect the stability of nano-fluids is the phenomenon of cluster formation or accumulation of particles that causes the deposition of these particles. To investigate the settling time, a mixture of nano-fluid Al₂O₃ + H₂O with a volume fraction of 1% of 20 nm nanoparticles was prepared. In order to prepare a completely homogeneous mixture, an electric mixer was used in the first experiment and in the second experiment, after preparing the mixture, it was mixed for 10 minutes on a magnetic shaker at a temperature of 30° C. Then 100 ml of the mixture was poured into a graduated container and photographed at specified intervals.

The results show that the use of electric mixer and then magnetic mixer to mix the nano-fluid makes the nano-fluid more stable. The results show a relative agreement with the source [23]. In order to maintain the stability of the solution to be suitable for engineering works, 1% by weight of sodium dodecyl benzene sulfonate (SDBS) was used for Al₂O₃ + H₂O as the sulfatcant. Al₂O₃ + H₂O was stable for the first 22 days and then began to be unstable.

Investigation of zeta potential

One of the most important methods to find the quality of nano-fluid stability is to study the kinetic behavior of particles in a colloidal solution due to the flow of electricity. According to a stability theory, if the zeta potential has a high absolute value, the electrostatic repulsion between the particles increases, which results in good suspension stability. Particles with high surface charge do not tend to form clusters. Many researchers, including Wu et al. [42], have reported that colloidal solutions are stable at zeta potentials greater than 30 mV. Zeta potential analyzer ZETA-

Check model made by German Particle Metrix Company was used to measure zeta potential. For this purpose, 2 wt% nanoparticles Al₂O₃ with a diameter of 20 nm were used. In this experiment, the temperature was 25 ° C, the pressure of one atmosphere and the humidity was 38%. The highest measured value for nano-fluid Al₂O₃ + H₂O was 37.7 mv, which indicates excellent stability and dispersion.

Thermal Conductivity Coefficient

Comparison of laboratory thermal conductivity coefficient with theoretical models

Al₂O₃ nano-fluid was tested with volume percentages of 1, 2, 3 and 4, then these values were recalculated and evaluated through 7 theories. With increasing the volume fraction of nanoparticles, the thermal conductivity coefficient of nano-fluids increased. The percentage of this increase is obtained from equation 15.

$$\%K_{enhancement} = \left[\frac{K_{nf} - K_{bf}}{K_{bf}} \right] \times 100 \quad (15)$$

In relation 15, nf index was used for nano-fluid and bf for base fluid.

Experimental data and theoretical outputs, the thermal conductivity coefficient indicates an increase in the heat transfer coefficient with increasing volume fraction. In this analysis, the Loo-Lin theory predicts the minimum, and the Pak-Cho theory predicts the maximum value for increasing the thermal conductivity coefficient (Fig. 4)

Investigating the influence of nanoparticles diameter on nanofluid thermal conductivity coefficient

The thermal conductivity coefficient of Al₂O₃ nanofluid was investigated at 1 to 4% volumetric rates for nanoparticles of 6, 10 and 20 nm, and the results are shown in Fig. 5. The results show that the smaller the diameter of the nanoparticles suspended in the base fluid, the more the thermal conductivity will increase. This is due to their surface-to-volume ratio, which by decreasing the size of the nanoparticles, more surface of it will be in thermal contact with the fluid. For example when the nanoparticle diameter was reduced from 20 nm to 10 nm. The thermal conductivity coefficient for volume fractions of 1 to 4% showed an average increase of 7%.

Investigation of changes in thermal conductivity coefficient of nanofluids with volume fraction of nanoparticles

Thermal conductivity coefficient of Al₂O₃ + H₂O was investigated in 1% to 5% volumetric percentages of nanoparticles. The results are shown in Fig. 6. The effect of volume fraction is incremental, which can be linear or nonlinear, and this increase occurs for different systems with different gradients. The reason for this issue is that the thermal conductivity coefficient nanofluids depend on both the thermal conductivity coefficient of the base fluid and the thermal conductivity coefficient of the nanoparticles. The obtained data were compared with the

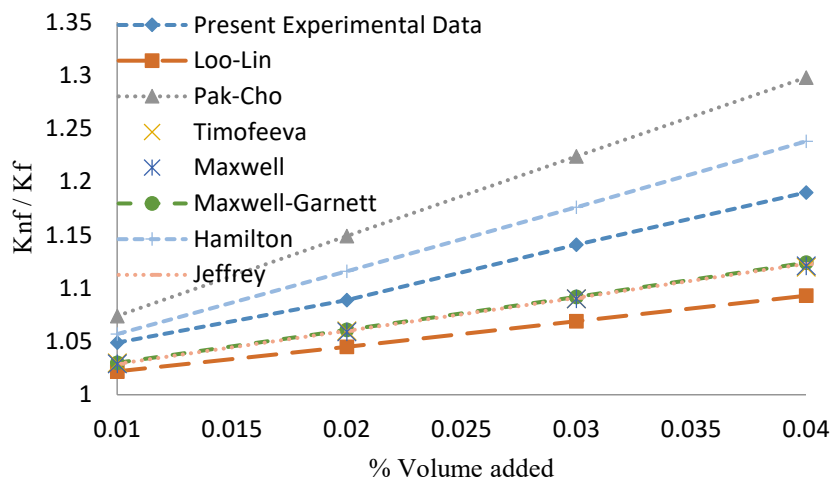


Fig. 4. Changes of theoretical heat transfer coefficient with volume fraction change (Al₂O₃+H₂O)



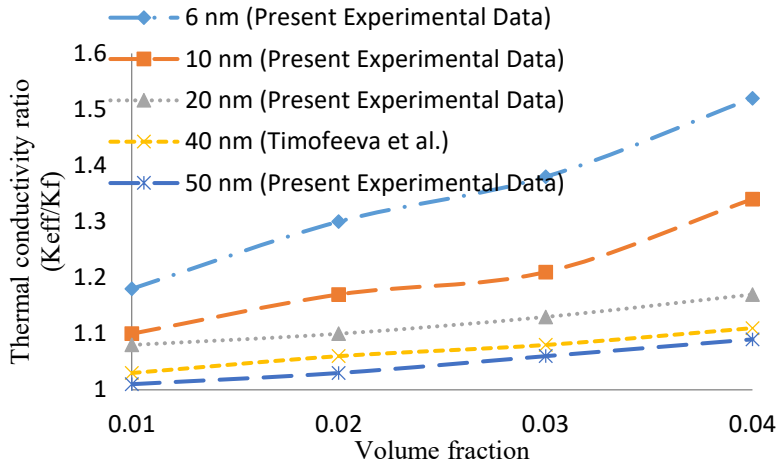


Fig. 5. Influence of nanoparticles size in different volume fraction on effective thermal conductivity of Al₂O₃+H₂O

research data of Lee et al. [27] and approximate concordance between the obtained results and the source results [27] is observed.

Investigation of the effect of temperature at different volume percentages on thermal conductivity coefficients

Al₂O₃ nanofluid with diameter of 20 nm was tested in volume fractions up to 4% and in the temperature range of 20 to 50 ° C and its thermal

conductivity coefficient was carefully measured and recorded. The results show that at lower volume fractions, the temperature difference has no significant effect on the thermal conductivity coefficient and the differences are little. But by increasing volume fraction, the effect of temperature on the heat transfer coefficient increases and peak of volume fraction 0.04. The reason for this issue can be considered in the increase in collisions between fluid molecules and

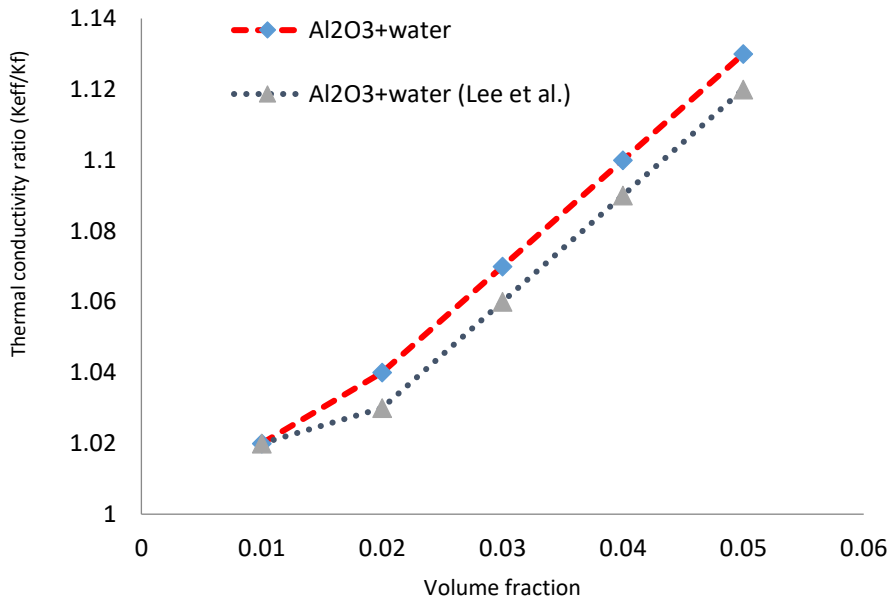


Fig. 6. Investigation of changes of thermal conductivity coefficient of Al₂O₃+H₂O nanofluid with volume fraction of nanoparticles

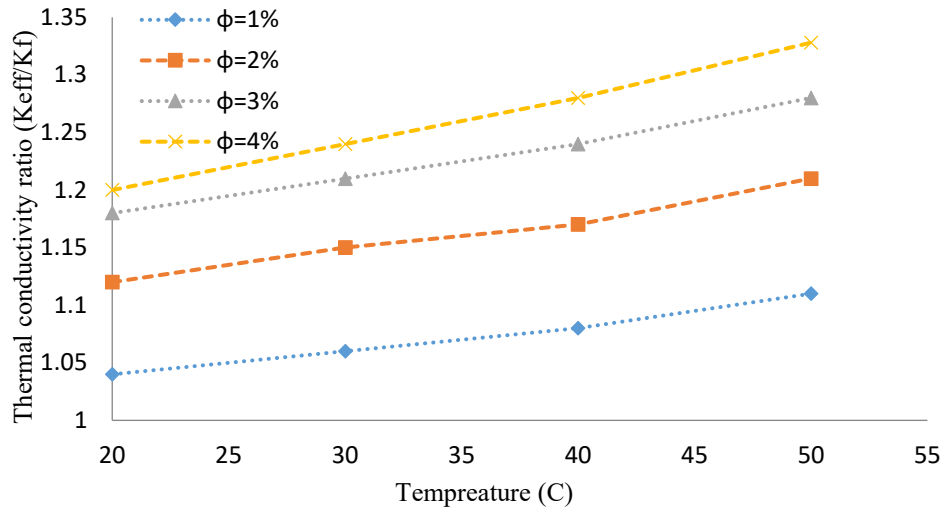


Fig. 7. Investigation of changes in thermal conductivity of nano-fluids $Al_2O_3 + H_2O$ with temperature changes in different volume fractions

suspended particles by increasing temperature. As the volume fraction increases, the number of particles in the base fluid increases, and the high temperature increases the speed of the collision of molecules and the Brownian motion.

A comparison with source [28] was performed to investigate the accuracy of the obtained numbers for 0.01 and 0.04 volume at temperatures between 20 and 50 ° C. Investigation of changes in thermal conductivity coefficient of nano-fluid $Al_2O_3 + H_2O$ was used with temperature changes in different volume fractions of nanoparticles with

a diameter of 20 nm. The results showed that with increasing temperature, at higher volume fractions, the effect of temperature on the thermal conductivity of nano-fluids is more tangible. With increasing temperature from 20 to 50 ° C for volume fractions of 1 to 4%, 7.6%, 8%, 8.4 and 9% increase in nano-fluid thermal conductivity was observed, respectively. Changes in the thermal conductivity of the nano-fluid were recorded at 20 ° C with increasing the volume fraction from 1 to 4% the lowest (15%) and at 50 ° C with increasing the volume fraction from 1 to 4% the highest

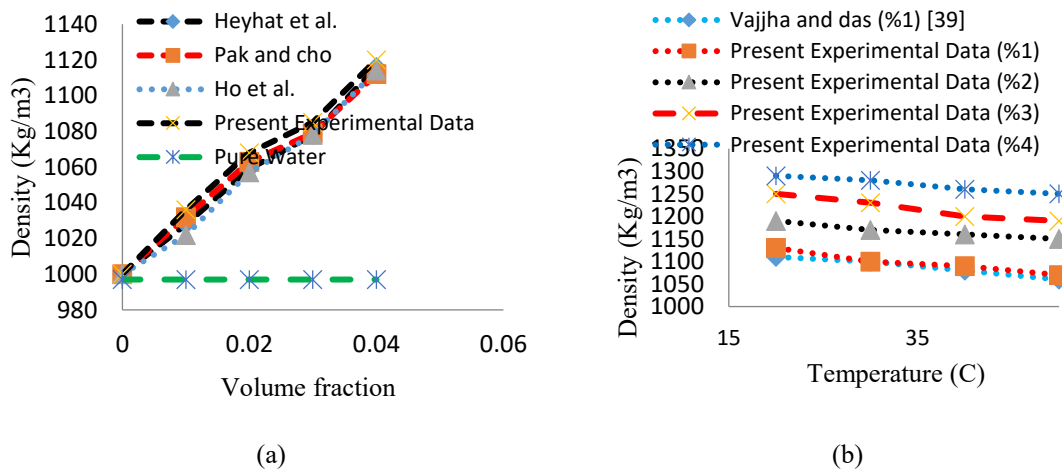


Fig. 8. (a) Density changes with volume fraction of nanoparticles, (b) Changes of $Al_2O_3+H_2O$ nanofluid density with changes of temperature for 1 to 4% volume fractions

(19%) (Fig. 7).

Comparison of thermal conductivity coefficient Al_2O_3 with basic fluids of water and ethylene glycol

By mixing the nanoparticles Al_2O_3 in two well-known base fluids, i.e water and ethylene glycol, we try to investigate the thermal conductivity coefficient of the nanofluid. Research shows that the more the selected fluid in terms of thermal properties is stronger; the impact of the nanoparticles on its thermal conductivity coefficient will be more. For the sample at 30 ° C, the thermal conductivity coefficient of ethylene glycol is 0.28 and for water is 0.62. If we examine the combination of the two with Al_2O_3 , we find that the thermal conductivity coefficient is lower in the combination of ethylene glycol with Al_2O_3 than its combination with water.

Investigation of density and specific heat of nano-fluid $Al_2O_3 + H_2O$

The density of nano-fluid in volume fractions between 1 to 4% was calculated using the digital portable density meter model DA130N of KEM

Company of Japan. The results show that the density of nanofluids is much higher than the base fluid density of water. And as the volume fraction of nanoparticles in nanofluid increases, the density increases. For example, by increasing the volume fraction from 3 to 4%, the nano-fluid density increased by 3.2%.

The results were compared with sources [25], [32] and [33]. Increasing the temperature causes the expansion in liquids and consequently the change in density (Fig. 8). All liquids don't expand at the same rate. In the next experiment, the changes of nanofluid density with temperature changes were investigated. The results showed that the density decreases by increasing temperature. But this reduction is not only dependent on temperature but also dependent on the volume fraction of nanoparticles suspended in the nanofluid. The results were evaluated with reference [34]. For example, at a volume percentage, the density decreased by 5.3% with increasing temperature from 20 to 50 ° C.

Prasher and his colleagues on a study conducted on Cuo / H_2O nanoparticles, found that

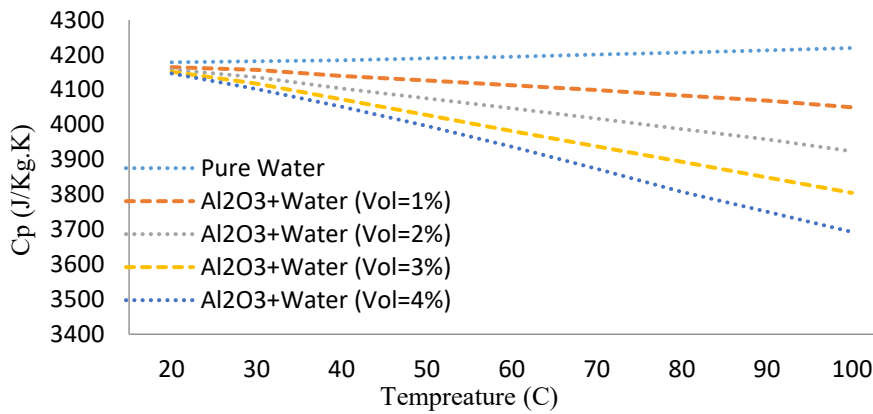


Fig. 9. Specific heat changes of water-based fluid and nano-fluid $Al_2O_3 + H_2O$ with respect to temperature

Table. 3. Thermo-physical properties of base fluids and nanoparticles [26].

Properties	Al_2O_3	Ethylene glycol	Water
$c_p(Jkg^{-1}K^{-1})$	765	2420.6	4179
$\rho(kgm^{-3})$	3970	1110.2	997.1
$K(Wm^{-1}k^{-1})$	40	0.253	0.613
$\beta \times 10^{-5}(k^{-1})$	0.85	57	21

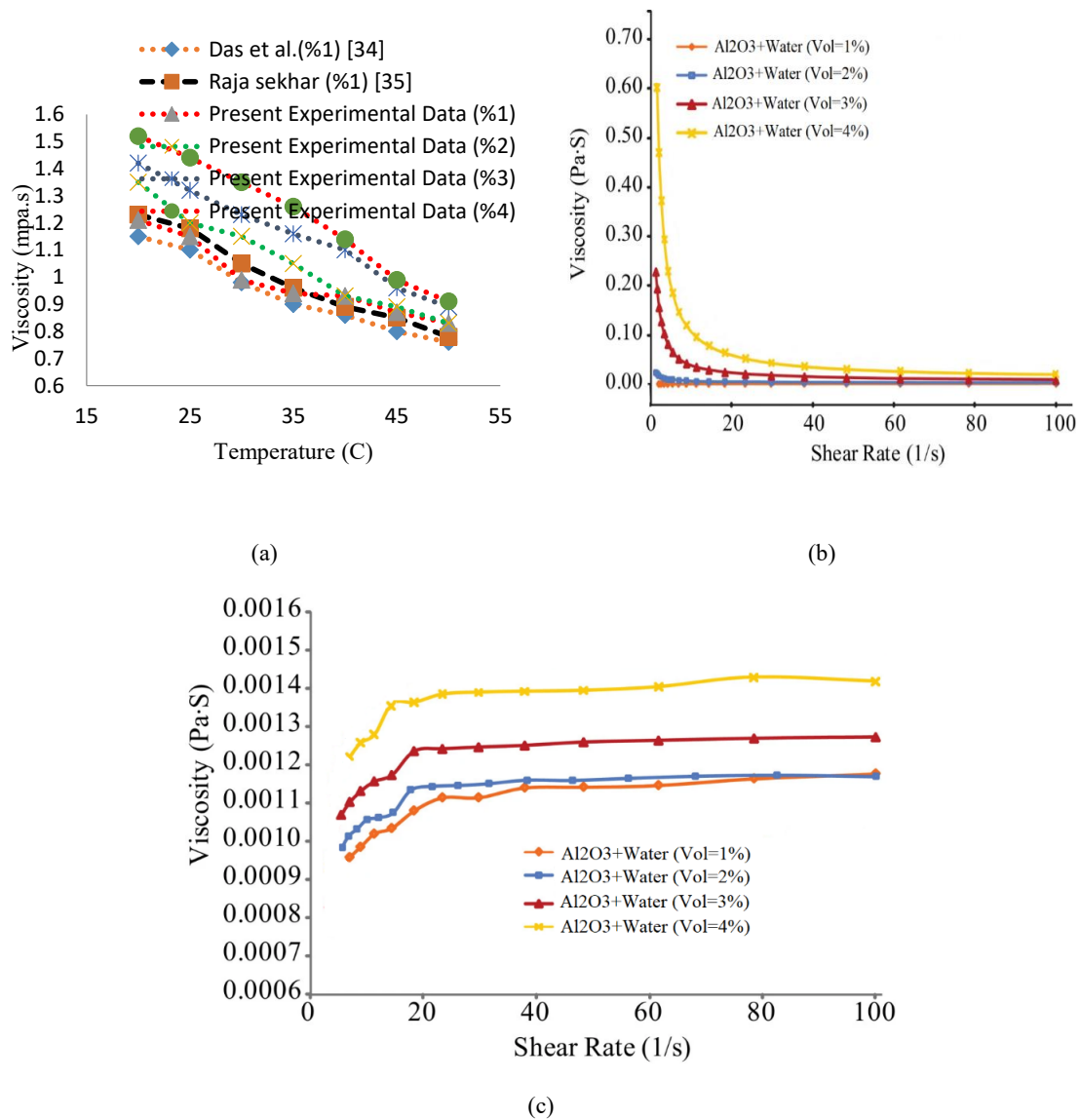


Fig. 10. (a) Viscosity changes of $Al_2O_3+H_2O$ nanofluid with temperature changes, (b) Viscosity changes relative to shear rate for volume fractions of 1 to 4% after 12 days, (c) Viscosity changes relative to shear rate for volume fractions of 1 to 4% after ultrasonic application

by increasing the density of nanoparticles inside the nanofluid due to increase inertia and reduce moving power of nanoparticles in the nanofluid, the heat transfer through Brownian motion was reduced [35]. The KD2-Pro was used to measure specific heat. The experiment was performed between 20 and 100 ° C. During this temperature range, the specific heat of water increased by 0.9%. But in the same heat range for volume fractions of 1 to 4%, a decrease of 2.7%, 5.5%, 8.3% and 10.9%

in specific heat was observed (Fig. 9).

Investigating nanofluid viscosity

Nanoparticles with diameter of 20 nm were used to measure the viscosity of Al_2O_3 nanofluid. Since the viscosity measurement is carried out at different temperatures, first, we set the viscometer bath on the considered temperature and gave the bath time to reach the test temperature. Then, we poured the nanofluid into a test tube

and placed it completely in the bath. Then, we waited for ten minutes to the bath temperature to be the same as the sample temperature. Then, we did the experiment. One of the parameters that affect the viscosity is temperature. As the temperature increases, the viscosity of the gases increases but the viscosity of the fluids decreases. This difference can be explained by examining the viscosity factors. The results were evaluated with the results of sources [30] and [31].

An average of at least 30% and a maximum of 40% decrease in viscosity was observed with increasing temperature from 20 to 50 ° C for volume fractions of 1 to 4%.

After 12 days of nano-fluid preparation, the changes in viscosity relative to the cutting rate for volume fractions of 1 to 4% were calculated. As shown in Fig. 10, in all volume fractions, the changes in viscosity with the shear rate are quite noticeable. At a given shear rate, nano-fluids with a volume fraction of 1% have the lowest and nano-fluids with a volume fraction of 4% have the highest viscosity. The dependence of the amount of viscosity on the shear rate also indicates the non-Newtonian behavior of the nano-fluid studied in the present study.

Then, after 12 days of preparation of nano-fluid, ultrasonic was used in order to redistribute the nanoparticles in the base fluid. Then the changes in viscosity relative to the cutting rate for volume fractions of 1 to 4% were calculated. The volume fractions showed the lowest 1% and the highest

4% increase in viscosity compared to the cutting rate. Up to a cut-off rate of $20 S^{-1}$ in all volume fractions is non-Newtonian fluid behavior and then tends to show Newtonian behavior.

Surface tension check

Tensiometer KRUSS K11 was used to measure surface tension. The concentration, temperature and diameter of nanoparticles affect the amount of surface tension. Surface tension decreases with increasing concentration and temperature because increasing molecular motion reduces the effect of intermolecular gravitational forces. For example, in the volume fraction of 4%, with increasing temperature from 20 to 50 ° C, the surface tension decreased by approximately 7.6%. Or at 50 ° C, with increasing volume fraction from 1% to 4%, surface tension decreased by 5.6% (Fig. 11).

In order to investigate the effect of nanoparticle diameter on surface tension, nanoparticles with a diameter of 20 nm and 40 nm were used. The results showed that with increasing the diameter of nanoparticles, surface tension increases. For example, at a volume fraction of 4%, with increasing nanoparticle diameter from 20 nm to 40 nm, surface tension increased by approximately 2.3% (Fig. 11).

Investigation of boiling point of nano-fluid

In order to investigate the boiling point of base fluid and nano-fluid with volume fractions of 1 to

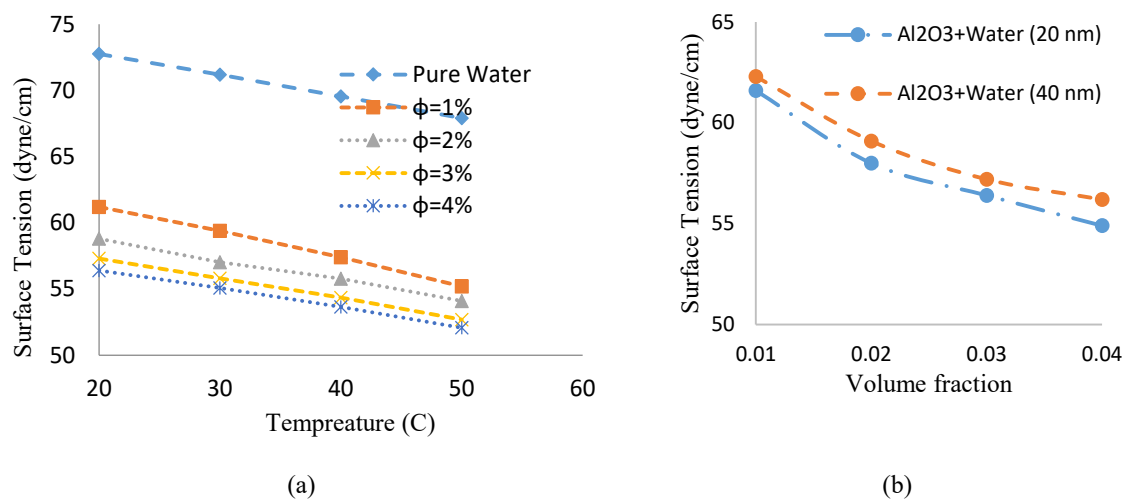


Fig. 11. (a) Changes in the surface tension of water-based fluid and nano-fluid with different volume fractions exposed to air, (b) Changes in the nanoparticle diameter on surface tension



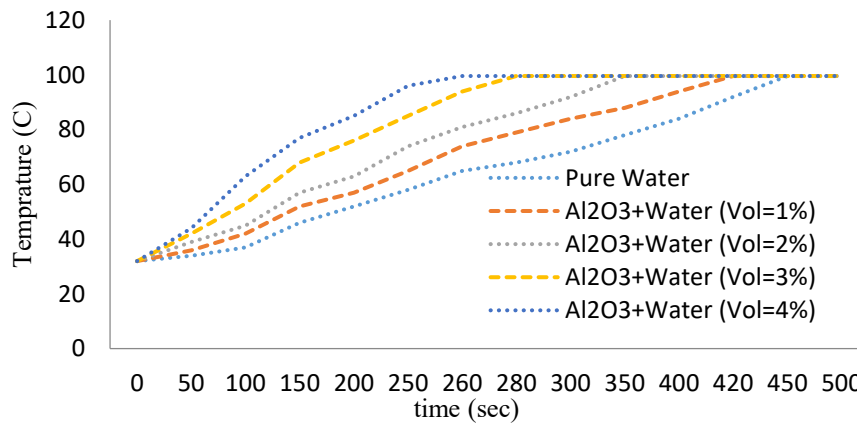


Fig. 12. Boiling point temperature for water-based fluid and nano-fluid $Al_2O_3 + H_2O$ in different volume fractions

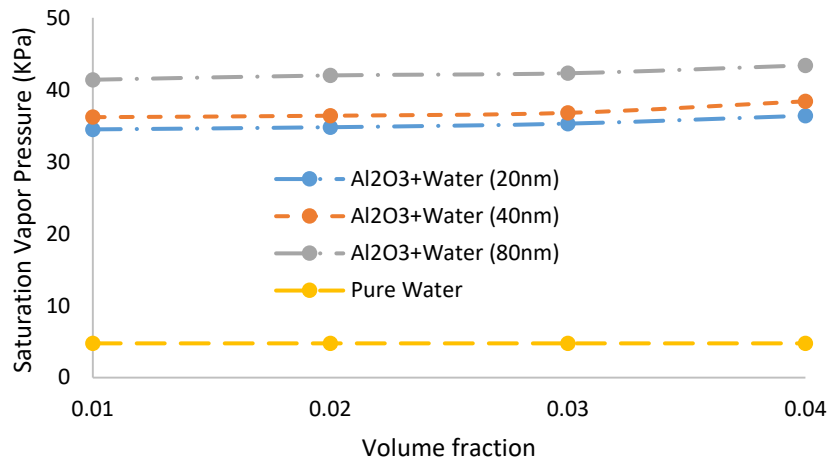


Fig. 13. Saturated steam pressure changes with volume fraction and nanoparticle diameter

4%, the oven of Shimi Fan Company was used. The TMP-10 temperature sensor has a measurement accuracy of ± 1 °C (0→150 °C). To test 300 ml of the test fluid was placed in an oven at ambient temperature (32 °C) and a pressure of 764 mm Hg, and the time required to boil was measured. According to Fig. 12, it can be seen that the slope of the heating curve (dT / dt) increases with increasing concentration of nanoparticles in the base fluid.

Measurement of saturated steam pressure

At 32 °C, saturated water steam pressure and nano-fluid with three different diameters were measured in volume fractions of 1 to 4%. The results showed that with increasing volume

fraction and nanoparticle size, saturated steam pressure increases. With increasing the volume fraction from 1% to 4% in 20 nm, 40 nm and 80 nm, respectively, an increase of 5.5%, 6% and 4.8% was observed (Fig. 13).

CONCLUSION

In the present study, Al_2O_3 nanoparticles in water-based fluids and ethylene glycol were mixed with 4% by volume (1.4%) using an electric mixer and a magnetic shaker. The stability of nano-fluids is still a challenging issue, and sulfate must be added to them to produce functional fluids. By adding SDBS surfactant to Al_2O_3 , the produced nano-fluid was stable for the first 22 days. Also, the value of zeta potential was estimated to be

37.7 mv, which indicates the stability of the nano-fluid. The results showed that with increasing the volume fraction of nanoparticles in the base fluid, the thermal conductivity coefficient, density, steam pressure and slope of the heating curve increase and the surface tension decreases. With increasing temperature, thermal conductivity and specific heat of water increased and density, viscosity and specific heat of nano-fluid decreased with different volume fractions. For example, with increasing temperature from 20 to 100 ° C, the specific heat of water increased by 0.9%. In the same temperature range for volume fractions of 1 to 4%, a decrease of 2.7%, 5.5%, 8.3% and 10.9% in specific heat was observed, respectively. Also, with increasing the diameter of nanoparticles, the thermal conductivity decreases and the surface tension of the nano-fluid increases. The practical thermal conductivity coefficient obtained was compared with the values of the prediction models of this coefficient. Based on the regression obtained for the calculated experimental results (R = 0.99), this value is consistent with the Timofeeva model. The stronger the thermal properties of the base fluid, the greater the effect on the thermal conductivity of the nano-fluid. Since increasing the temperature of nano-fluids increases the thermal conductivity, it can be concluded that their application in higher temperature environments is beneficial.

CONFLICT OF INTEREST

The authors declare that there is no conflict of interests regarding the publication of this manuscript.

REFERENCES

1. Fluid Particles in Non-Newtonian Media. Bubbles, Drops, and Particles in Non-Newtonian Fluids: CRC Press; 2006. p. 231-306.
2. Masuda H, Ebata A, Teramae K, Hishinuma N. Alteration of Thermal Conductivity and Viscosity of Liquid by Dispersing Ultra-Fine Particles. Dispersion of Al₂O₃, SiO₂ and TiO₂ Ultra-Fine Particles. *Netsu Bussei*. 1993;7(4):227-233.
3. Das SK, Choi SUS, Yu W, Pradeep T. *Nanofluids*: John Wiley & Sons, Inc.; 2007 2007/07/12.
4. Jwo C-S, Jeng L-Y, Teng T-P, Chen C-C. Performance of overall heat transfer in multi-channel heat exchanger by alumina nanofluid. *Journal of Alloys and Compounds*. 2010;504:S385-S388.
5. *Dynamic Light Scattering*. Springer US; 1985.
6. Esmaeilzadeh E, Almohammadi H, Nasiri Vatan S, Omrani AN. Experimental investigation of hydrodynamics and heat transfer characteristics of γ-Al₂O₃/water under laminar flow inside a horizontal tube. *International Journal of Thermal Sciences*. 2013;63:31-37.
7. Peyghambarzadeh SM, Hashemabadi SH, Jamnani MS, Hoseini SM. Improving the cooling performance of automobile radiator with Al₂O₃/water nanofluid. *Appl Therm Eng*. 2011;31(10):1833-1838.
8. Teamah MA, El-Maghlany WM. Augmentation of natural convective heat transfer in square cavity by utilizing nanofluids in the presence of magnetic field and uniform heat generation/absorption. *International Journal of Thermal Sciences*. 2012;58:130-142.
9. Zeitoun O, Ali M. Nanofluid impingement jet heat transfer. *Nanoscale Research Letters*. 2012;7(1).
10. Anbumozhi Angayarkanni S, Philip J. Role of surface charge, morphology, and adsorbed moieties on thermal conductivity enhancement of nanofluids. *Applied Physics Letters*. 2012;101(17):173113.
11. Sundar LS, Sharma KV, Naik MT, Singh MK. Empirical and theoretical correlations on viscosity of nanofluids: A review. *Renewable and Sustainable Energy Reviews*. 2013;25:670-686.
12. Mena JB, Ubices de Moraes AA, Benito YR, Ribatski G, Parise JAR. Extrapolation of Al₂O₃-water nanofluid viscosity for temperatures and volume concentrations beyond the range of validity of existing correlations. *Appl Therm Eng*. 2013;51(1-2):1092-1097.
13. Mostafizur RM, Abdul Aziz AR, Saidur R, Bhuiyan MHU, Mahbubul IM. Effect of temperature and volume fraction on rheology of methanol based nanofluids. *International Journal of Heat and Mass Transfer*. 2014;77:765-769.
14. Khodaei M, Enayati MH, Karimzadeh F. Mechanochemical behavior of Fe₂O₃-Al-Fe powder mixtures to produce Fe₃Al-Al₂O₃ nanocomposite powder. *JMatS*. 2007;43(1):132-138.
15. Hemmat Esfe M, Karimipour A, Yan W-M, Akbari M, Safaei MR, Dahari M. Experimental study on thermal conductivity of ethylene glycol based nanofluids containing Al₂O₃ nanoparticles. *International Journal of Heat and Mass Transfer*. 2015;88:728-734.
16. Hemmat Esfe M, Saedodin S. An experimental investigation and new correlation of viscosity of ZnO-EG nanofluid at various temperatures and different solid volume fractions. *Exp Therm Fluid Sci*. 2014;55:1-5.
17. Turkyilmazoglu M. Analytical solutions of single and multi-phase models for the condensation of nanofluid film flow and heat transfer. *European Journal of Mechanics - B/ Fluids*. 2015;53:272-277.
18. Mierczynski P. Comparative Studies of Bimetallic Ru-Cu, Rh-Cu, Ag-Cu, Ir-Cu Catalysts Supported on ZnO-Al₂O₃, ZrO₂-Al₂O₃ Systems. *Catalysis Letters*. 2016;146(10):1825-1837.
19. Maxwell JC. *A Treatise on Electricity and Magnetism*: Cambridge University Press; 2010 2010/06/24.
20. XII. Colours in metal glasses and in metallic films. *Philosophical Transactions of the Royal Society of London Series A, Containing Papers of a Mathematical or Physical Character*. 1904;203(359-371):385-420.
21. Hamilton RL, Cresser OK. Thermal Conductivity of Heterogeneous Two-Component Systems. *Industrial & Engineering Chemistry Fundamentals*. 1962;1(3):187-191.
22. Conduction through a random suspension of spheres. *Proceedings of the Royal Society of London A Mathematical and Physical Sciences*. 1973;335(1602):355-367.
23. Lu SY, Lin HC. Effective conductivity of composites containing aligned spheroidal inclusions of finite conductivity. *Journal*

- of Applied Physics. 1996;79(9):6761-6769.
24. Timofeeva EV, Gavrilov AN, McCloskey JM, Tolmachev YV, Sprunt S, Lopatina LM, et al. Thermal conductivity and particle agglomeration in alumina nanofluids: Experiment and theory. *PhRvE*. 2007;76(6).
25. Pak BC, Cho YI. HYDRODYNAMIC AND HEAT TRANSFER STUDY OF DISPERSED FLUIDS WITH SUBMICRON METALLIC OXIDE PARTICLES. *ExHT*. 1998;11(2):151-170.
26. Wen D, Lin G, Vafaei S, Zhang K. Review of nanofluids for heat transfer applications. *Particuology*. 2009;7(2):141-150.
27. Lee S, Choi SUS, Li S, Eastman JA. Measuring Thermal Conductivity of Fluids Containing Oxide Nanoparticles. *J Heat Transfer*. 1999;121(2):280-289.
28. Das SK, Putra N, Thiesen P, Roetzel W. Temperature Dependence of Thermal Conductivity Enhancement for Nanofluids. *J Heat Transfer*. 2003;125(4):567-574.
29. Khedkar RS, Sonawane SS, Wasewar KL. Influence of CuO nanoparticles in enhancing the thermal conductivity of water and monoethylene glycol based nanofluids. *ICHMT*. 2012;39(5):665-669.
30. Das SK, Putra N, Roetzel W. Pool boiling characteristics of nano-fluids. *International Journal of Heat and Mass Transfer*. 2003;46(5):851-862.
31. Sekhar YR, Sharma KV. Study of viscosity and specific heat capacity characteristics of water-based Al_2O_3 nanofluids at low particle concentrations. *J Exp Nanosci*. 2013;10(2):86-102.
32. Heyhat MM, Kowsary F, Rashidi AM, Alem Varzane Esfehiani S, Amrollahi A. Experimental investigation of turbulent flow and convective heat transfer characteristics of alumina water nanofluids in fully developed flow regime. *ICHMT*. 2012;39(8):1272-1278.
33. Ho CJ, Liu WK, Chang YS, Lin CC. Natural convection heat transfer of alumina-water nanofluid in vertical square enclosures: An experimental study. *International Journal of Thermal Sciences*. 2010;49(8):1345-1353.
34. Vajjha RS, Das DK. Experimental determination of thermal conductivity of three nanofluids and development of new correlations. *International Journal of Heat and Mass Transfer*. 2009;52(21-22):4675-4682.
35. Prasher R, Bhattacharya P, Phelan PE. Thermal Conductivity of Nanoscale Colloidal Solutions (Nanofluids). *Physical Review Letters*. 2005;94(2).
36. Leong KY, Saidur R, Kazi SN, Mamun AH. Performance investigation of an automotive car radiator operated with nanofluid-based coolants (nanofluid as a coolant in a radiator). *Appl Therm Eng*. 2010;30(17-18):2685-2692.
37. Turgut A, Tavman I, Chirtoc M, Schuchmann HP, Sauter C, Tavman S. Thermal Conductivity and Viscosity Measurements of Water-Based TiO_2 Nanofluids. *International Journal of Thermophysics*. 2009;30(4):1213-1226.
38. Bahiraei M, Hosseinalipour SM, Zabihi K, Taheran E. Using Neural Network for Determination of Viscosity in Water- TiO_2 Nanofluid. *Advances in Mechanical Engineering*. 2012;4:742680.
39. Fan X, Chen H, Ding Y, Plucinski PK, Lapkin AA. Potential of 'nanofluids' to further intensify microreactors. *Green Chem*. 2008;10(6):670.
40. Ghadimi A, Metselaar IH. The influence of surfactant and ultrasonic processing on improvement of stability, thermal conductivity and viscosity of titania nanofluid. *Exp Therm Fluid Sci*. 2013;51:1-9.
41. Yiamsawas T, Dalkilic AS, Mahian O, Wongwises S. Measurement and Correlation of the Viscosity of Water-Based Al_2O_3 and TiO_2 Nanofluids in High Temperatures and Comparisons with Literature Reports. *Journal of Dispersion Science and Technology*. 2013;34(12):1697-1703.
42. Wu S, Zhu D, Li X, Li H, Lei J. Thermal energy storage behavior of $Al_2O_3-H_2O$ nanofluids. *Thermochim Acta*. 2009;483(1-2):73-77.
43. Kong L, Sun J, Bao Y. Preparation, characterization and tribological mechanism of nanofluids. *RSC Advances*. 2017;7(21):12599-12609.
44. Ghiyasiyan-Arani M, Salavati-Niasari M, Zonouz AF. Effect of Operational Synthesis Parameters on the Morphology and the Electrochemical Properties of 3D Hierarchical AlV_3O_9 Architectures for Li-Ion Batteries. *Journal of The Electrochemical Society*. 2020;167(2):020544.
45. Farahani SD, Farahani M, Ghanbari D. Heat transfer from R134a/oil boiling flow in pipe: Internal helical fin and hybrid nanoparticles. *Chem Eng Res Des*. 2021;175:75-84.